Applied Catalysis B: Environmental 165 (2015) 117–127

Contents lists available at ScienceDirect

Applied Catalysis B: Environmental

journal homepage: www.elsevier.com/locate/apcatb

Steam reforming of cyclic model compounds of bio-oil over Ni-based catalysts: Product distribution and carbon formation

R. Trane-Restrup, A.D. Jensen*

Department of Chemical and Biochemical Engineering, Technical University of Denmark, Søltofts Plads, Building 229, 2800 Kgs. Lyngby, Denmark

ARTICLE INFO

Article history:
Received 7 July 2014
Received in revised form 4 September 2014
Accepted 12 September 2014
Available online 2 October 2014

Keywords:
Steam reforming
Carbon deposition
Furfural
2-Methylfuran
Guaiacol

ABSTRACT

Steam reforming (SR) and oxidative steam reforming (OSR) of furfural, 2-methylfuran, and guaiacol have been investigated in the temperature range 400–800 °C at a steam to carbon (S/C)-ratio of 5 and oxygen to carbon (O/C)-ratio of 0.2–1.4 over Ni/CeO_2-K/$MgAl_2O_4$. Carbon oxides and H_2 were the major products in the SR of 2-methylfuran and furfural, while the by-products were methane, ethanol, 2-propanol, and acetone. Temperatures of 500 °C or above were needed to minimize the formation of by-products in the SR of 2-methylfuran and furfural. Phenolics, like benzenediols and phenol, were produced in high yields in the SR of guaiacol and temperatures of 780 °C were needed to totally convert guaiacol to carbon oxides and H_2.

Carbon deposition was observed in the SR of all three model compounds and was most severe for guaiacol followed by furfural and 2-methylfuran. The carbon deposition could be reduced significantly by adding oxygen to the feed at a cost of a lower yield of H_2. Stable operation was observed initially (first 4 h) in the OSR of all compounds, but experiments over 24 h showed signs of deactivation due to an accelerated rate of carbon deposition in the SR of furfural and guaiacol. Furthermore sintering was more severe in OSR.

1. Introduction

Biomass constitutes one of the few renewable carbon sources and therefore utilization of biomass for production of fuels or chemicals has received much attention in the recent decades [1,2]. Furthermore, biomass has the potential to be CO_2-neutral and so chemicals or fuels produced from biomass generally are considered sustainable. One of the problems with biomass as a raw material is a low energy density, which makes transportation of it costly [3]. A possible solution to this problem is to do a local or even on site flash pyrolysis of biomass, which yields a liquid fraction, called bio-oil, as well as a gaseous and solid char fraction [3–5]. The gas fraction can provide energy for the pyrolysis process, while the char can be used as fertilizer and soil improver [5,6]. The bio-oil can be produced in yields up to 75% with an energy density up to ten times higher compared with untreated biomass decreasing the costs of transportation [3–5,7].

Bio-oil is a mixture of many different oxygenates ranging from acetic acid to aromatics like guaiacol and sugar derived compounds such as levoglucosan [5,7–10]. The oil is acidic and has a low heating value compared to fossil fuels. Furthermore the bio-oil is not stable over time as the oxygenates can react with other compounds in the oil leading to an increase in viscosity and average molar weight and in severe cases the bio-oil may phase separate into aqueous and organic fractions [8–10]. Thus, bio-oil is not suited for combustion in most engines and so catalytic upgrading of the bio-oil by either hydrodeoxygenation (HDO) or steam reforming (SR) is needed [1,11,12].

Steam reforming of bio-oil can be used in biorefineries or integrated into conventional oil refineries to supply H_2 or synthesis gas for processes like hydrotreating, ammonia, methanol, or Fischer–Tropsch synthesis. One of the main challenges in SR of bio-oil and other oxygen containing hydrocarbons is deactivation of catalysts mainly due to carbon deposition [12–16]. Therefore optimization of the catalyst has been attempted by changing support [17–19], alloying different metals [20–23], using noble metals [14,24,25], or adding promoters [17,26–29]. CeO_2 and K are interesting promoters, as they can increase activity and decrease carbon deposition in the SR of ethanol due to an increased rate of oxidation/gasification of carbon or other surface reactions leading to lower surface coverage of carbon forming species [17,27–30].

Abbreviations: HDO, hydrodeoxygenation; LHSV, liquid hourly space velocity; OSR, oxidative steam reforming; SR, steam reforming; WGS, water gas shift.

* Corresponding author. Tel.: +45 4525 2841; fax: +45 4588 2258.
E-mail address: aj@kt.dtu.dk (A.D. Jensen).

http://dx.doi.org/10.1016/j.apcatb.2014.09.026
0926-3373/

Another option for lowering of the carbon deposition is the addition of oxygen to the feed, so called oxidative SR (OSR), which has shown promising results with stable behavior of the catalyst with time-on-stream and low rates of carbon deposition in the SR of ethanol [25,31–35], acetic acid [36] and bio-oil [13,37–39]. The penalty of oxygen addition is a lower yield of H_2.

The equilibrium product gas composition in the SR of oxygenates can be described by the equilibrium between SR, reaction (1), water gas shift (WGS), reaction (2), and methanation, reaction (3):

$$C_nH_mO_p + (n-p)H_2O \rightleftharpoons n\,CO + \left(n - p + \frac{m}{2}\right) H_2 \quad (1)$$

$$CO + H_2O \rightleftharpoons CO_2 + H_2 \quad (2)$$

$$CO + 3H_2 \rightleftharpoons CH_4 + H_2O \quad (3)$$

At temperatures below 500 °C the thermodynamically favorable products are CO_2 and CH_4, while the fraction of CO and H_2 will increase at the expense of CO_2 and CH_4 as the temperature increases. At temperatures above 800 °C the WGS will shift toward CO and H_2O and therefore the highest yield of H_2 is obtained at temperatures between 600 and 800 °C.

Carbon deposition can occur by methane decomposition, the Boudouard reaction, and CO decomposition [40], but ethene or other olefins may also lead to carbon deposition if they are formed as intermediates [17,41,42]. For example, ethene or others olefins may easily be formed from ethanol and other alcohols by dehydration [15,16,42,43]. Furthermore, thermal decomposition of the oxygenates in the gas phase can also lead to carbon formation, which might clog process equipment. The different carbon forming reactions are shown below.

$$\text{Boudouard}: 2CO \rightleftharpoons C_s + CO_2 \quad (4)$$

$$\text{CO decomposition}: CO + H_2 \rightleftharpoons C_s + H_2O \quad (5)$$

$$\text{CH}_4\ \text{decomposition}: CH_4 \rightleftharpoons C_s + 2H_2 \quad (6)$$

$$\text{Ethene polymerization}: n\,C_2H_4 \rightarrow \text{Carbon} \quad (7)$$

$$\text{Thermal decomposition}: C_nH_mO_p \rightarrow C_xH_yO_z + \text{gases} + \text{coke} \quad (8)$$

Steam reforming of bio-oil has been investigated with the entire oil fraction [13,37,44–51] or the aqueous fraction of bio-oil, formed by water addition to the bio-oil [38,52–56]. However, studies using model compounds of bio-oil may be used to obtain a better understanding of which species are the main cause of the observations made in SR of real bio-oils. There is a lack of studies with cyclic oxygenates as model compounds. These are present in the bio-oil and may be responsible for a significant fraction of the carbon deposition. The cyclic compounds in bio-oil can be divided into three main fractions, phenols, sugars, and furans. SR of sugars have been investigated previously [57–59] and therefore we chose to investigate SR of guaiacol, 2-methyl furan, and furfural. Guaiacol, which represents the phenols in the bio-oil, has been reported in concentrations from 0.2 to 5.32 wt%, while furans like 2-methylfuran and furfural have been reported in concentrations between 0.5 and 3.5 wt% [5,9,60,61].

Recently Xu et al. [62] studied the SR of several model compounds of bio-oil, including furfural and *m*-cresol, over Ni/MgO at 600 °C, S/C-ratio of 6, and liquid hourly space velocity (LHSV) of 5 h^{-1}. Their study focused on the type of by-products formed while the catalyst stability as well as the effect of temperature on product distribution was not investigated. Lan et al. [45] investigated the SR of furfural and *m*-cresol at S/C-ratio of 5 as function of temperature over several Ni/Al_2O_3 based catalysts and found that CO and CO_2 were the main products in the SR of furfural. Conversions above 90% was achieved at temperatures above 700 °C and LHSV of 2.5 h^{-1}. A stability test over 10 h showed a slight deactivation, but the source of deactivation was not investigated [45]. Recently Sayas and Chica [63] investigated the effect of the support material in SR of furfural and found that optimal support was natural sepiolite: furthermore acetone was reported as by-product. To the authors knowledge, there are no other published results on SR of furfural, guaiacol, and 2-methylfuran, which are all present in bio-oil. The aim of this work is therefore to investigate the SR of these compounds with focus on the product distribution as function temperature as well as function of time to investigate catalyst deactivation. Furthermore oxidative conditions are investigated to clarify what levels of O_2 are needed for stable operation.

2. Experimental

2.1. Catalyst preparation

Two catalysts were prepared by incipient wetness impregnation with a $Ni(NO_3)_2$-solution on two different carriers; $MgAl_2O_4$ (Puralox MG30/150 from Sasol, 143 m^2/g, pore volume: 0.9 mL/g) and CeO_2-K/$MgAl_2O_4$. The latter was prepared by impregnation of $MgAl_2O_4$ with an aqueous solution containing both $Ce(NO_3)_3{\cdot}6H_2O$ and KNO_3 followed by drying at 110 °C and calcination 800 °C (heating rate 10 °C/min) for 2 h. Ni was impregnated on both supports by dissolving $Ni(NO_3)_2{\cdot}6H_2O$ (Sigma–Aldrich, >97% pure) in a volume of water corresponding to the pore volume of the dry carrier. The solution was mixed with the dry carrier material and stirred. The wet powder was dried at 110 °C overnight and calcined at 800 °C (heating rate 10 °/min) for 2 h. The nominal loading of Ni, CeO_2, and K was 8 wt%, 5 wt%, and 5 wt%, respectively.

2.2. Experimental setup

The flowsheet of the experimental setup used in this study is shown in Fig. S.1 in the Supporting Information. The setup consisted of a gas supply section where up to eight different gases could be connected, a liquid supply section with a bubble column to supply water and a pump to supply the oxygenate. In the bubble column, a N_2 flow was saturated with water at 85 °C and led to the reactor. The N_2-steam mixture was transported in lines heated to 110 °C and mixed with a flow of oxygenate in N_2 prior to entering a quartz reactor placed in a three zone furnace. The effluent from the reactor passed through two condensers operated at 6–7 °C and −3 °C, respectively, which collected liquid H_2O, liquid products, and unconverted reactant. After the condensers the gases passed the analysis section, which consisted of a Varian MicroGC CP-4900 and a 5-channel Rosemount NGA 2000 on-line gas analyzer. The MicroGC had two columns, a molecular sieve 5A and a PoraPlot Q, and two thermal conductivity detectors (TCD), which measured the concentrations of CO, CO_2, H_2, CH_4, C_2H_4, C_2H_6, and C_3H_8. GC measurements were conducted every 10 min and representative measurements for every 30–60 min are used to show transient behavior. The on-line gas analyzer measured the CO, CO_2, and O_2 concentrations continuously based on IR measurements and data sets were collected every 30–60 s.

Analysis of the liquid from the condensers was conducted by a Shimadzu GCMS/FID-QP2010 UltraEi fitted with a Supelco Equity-5 column. Identification was made on the mass spectrometer (MS) and quantification was done on the flame ionization detector (FID).

The catalyst was placed between two pieces of quartz wool resting on a quartz frit inside a quartz tube with an inner diameter of 17 mm. The steam and oxygenate diluted in N_2 were fed from the top of the reactor through an inlet tube with an inner diameter of 4 mm and perforated with 12 holes in the end to disperse the gas over catalyst bed. A flow of N_2 or N_2 and O_2 were fed through a secondary inlet to the reactor and mixed with the steam-oxygenate

Table 1
Characterization results of the fresh catalysts (Ni as NiO) prepared by calcination in stagnant air at 800 °C. XRD reflection peak from NiO and CeO_2 at $2\theta = 62.8°$ and $2\theta = 47.5°$, respectively, were used for determination of particle sizes.

Catalyst	Promoter	Ni loading [wt%]	Surface area [m^2/g]	$d_{p,NiO}$ [nm]	d_{p,CeO_2} [nm]
$MgAl_2O_4$	–		143	–	–
$Ni/MgAl_2O_4$	–	8.2	104	5	–
Ni/CeO_2-K/ $MgAl_2O_4$	5 wt% CeO_2 5 wt% K	8.2	78	7	6

mixture at the outlet of the perforated inlet tube. This outlet was approx. 5 cm above the catalyst bed, which allowed for mixing of the gases prior to the catalyst bed. The temperature was measured by a thermocouple just below the quartz frit.

2.2.1. Catalytic test

0.5 g of catalyst with a particle size of 250–425 μm was loaded into the reactor resulting in a catalyst bed with a height of 3–4 mm. The reactor was heated to 600 °C in a flow of N_2 and the flow was changed to a 50/50 flow of N_2 and H_2 of roughly 500 NmL/min for 1 h at 600 °C to reduce the catalyst. TPR studies have shown that full reduction of the Ni occurs at these conditions [17]. After reduction, the reactor was purged with N_2 for 10 min and then the reactants were directed to the reactor. The general conditions were a total feed flow rate of about 1600 NmL/min with 1.0–1.5 vol% of oxygenate, roughly 35 vol% H_2O, various amounts of O_2 (0–4.8 vol%), and N_2 as balance.

The investigation of the influence of temperature was conducted without changing the catalyst sample and by staying for 2 h at each temperature from 700 °C to 400 °C to minimize the influence of carbon deposition which is more significant at low temperatures, 400 and 500 °C [17]. In the SR of guaiacol the order was 700-780-600-500-400 °C, because full conversion was not observed at 700 °C.

2.2.2. Determination of the amount of carbon deposited

The amount of carbon deposited during an experiment was determined by cooling the reactor to 200 °C and then heating the spent catalyst to 700 °C (10 °C/min) in a 1 NL/min flow of 2–3% O_2 in N_2. The evolution of CO and CO_2 was monitored by the online gas analyzer (data points every 5 s) and the amount of carbon in the reactor was determined by integration of these signals.

2.3. Catalyst characterization

The BET surface area of the prepared catalyst was measured by N_2 adsorption at its boiling point using multipoint BET theory with seven points in the $p/p_0 = 0.05$–0.3 range using a Quantachrome iQ2.

XRD-spectra of the fresh and spent catalysts were recorded by a PANalytical X'Pert PRO Diffractometer, which had a rotating sample holder, a rotating copper anode X-ray source, nickel filter, and automatic anti-scatter and divergence slits. NiO and CeO_2 particle sizes were determined from the line broadening in the XRD patterns using the Scherrer equation, Eq. (9) [64]:

$$d_p = \frac{K \cdot \lambda}{\beta \cdot \cos(\theta)} \tag{9}$$

K is a shape factor set to 0.9 [64], λ is the X-ray wavelength, β is full width at half maximum for the reflection peak corrected for the instrumental line broadening, while θ is the Bragg angle.

Bright field transmission electron microscopy of the spent catalysts were conducted on a Tecnai T20 G2 microscope with a thermionic-lanthanum hexaboride, LaB_6, as electron source. The spent catalysts were cooled down in N_2, removed from the reactor, and transported to TEM investigations. The samples for TEM were crushed, slurried with ethanol and deposited on a copper grid covered with a lacey carbon film.

2.4. Calculations

Conversion, X, is calculated on a carbon basis as:

$$X = \frac{\sum n_{C,i} \cdot n_i}{n_{C,Oxy} \cdot n_{Oxy,in}} \cdot 100\% \tag{10}$$

where $n_{C,i}$ is the number of carbon atoms in component i, n_i is the number of moles of compound i produced, and $n_{Oxy,in}$ is the molar flow of the model compound going into the system.

The product yields, Y_i, are defined as given by Fogler [65] based on the fraction of converted reactant:

$$Y_i = \frac{n_{C,i} \cdot n_i}{\sum n_{C,i} \cdot n_i} \cdot 100\% \tag{11}$$

The yield of H_2 is defined as:

$$Y_{H_2} = \frac{n_{H_2}}{n_{H_2,Max} \cdot X \cdot n_{Oxy,in}} \cdot 100\% \tag{12}$$

The factor of $n_{H_2,Max}$ is the maximum number of H_2 moles, which can be produced from 1 mol of oxygenate including full shift of CO to CO_2 and H_2. $n_{H_2,Max}$ is 12 for 2-methylfuran, 10 for furfural, and 16 for guaiacol.

Carbon deposition is reported as the amount of carbon deposited pr. amount carbon in the feed, mmol C/mol C_{Feed}, and in mass of carbon deposited pr. mass of catalyst and time, mg C/g_{Cat} h.

3. Results and discussion

3.1. Prereaction characterization

The surface areas of the fresh catalysts as well as the particle sizes of NiO and CeO_2 can be seen in Table 1. The surface area of Ni/CeO_2-K/$MgAl_2O_4$ was 78 m^2/g, while the NiO and CeO_2 particles had diameters of 7 nm and 6 nm, respectively. This was slightly higher compared with the NiO-particles on $MgAl_2O_4$, which was 5 nm in diameter. The loading of CeO_2 corresponded to roughly one monolayer, while the potassium loading was chosen based on the optimal value of 8 wt% K found by Hu and Lu [30]. Their catalyst however had a surface area of 125 m^2/g, thus we used about 5 wt% K to provide the same surface coverage of K. It corresponded to about two monolayers of K.

The XRD patterns of Ni/CeO_2-K/$MgAl_2O_4$ and $Ni/MgAl_2O_4$ are compared with the standard peaks for NiO, $MgAl_2O_4$, and CeO_2 in Fig. 1. Here it can be seen that NiO and $MgAl_2O_4$ accounts for the peaks in the XRD pattern of $Ni/MgAl_2O_4$, while the additional peaks in the XRD pattern of Ni/CeO_2-K/$MgAl_2O_4$ correspond to CeO_2. K was not observed in the XRD-pattern indicating that K is present as small crystallites or amorphous K.

3.2. Steam reforming of 2-methylfuran

Steam reforming of 2-methylfuran at S/C-ratio of 5 was carried out in an empty reactor to examine the extent of the homogenous reactions of 2-methylfuran. The conversion to gaseous products, CO, CO_2, CH_4, C_2- and C_3-hydrocarbons, was 3% at 700 °C and increased to 66% at 860 °C. Therefore homogeneous reactions were insignificant at the investigated temperatures. It should be noted

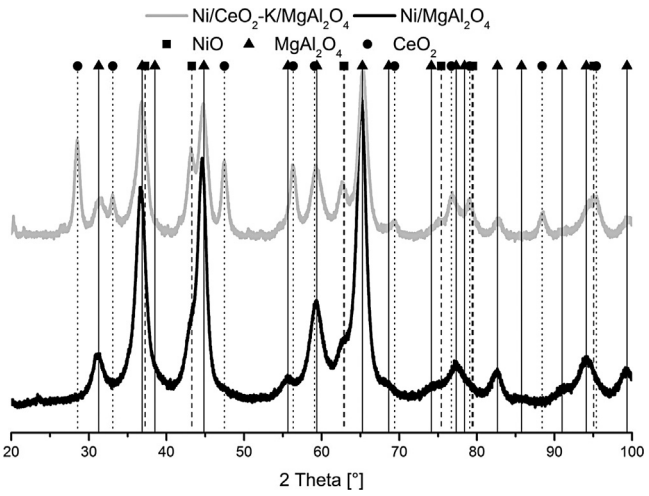

Fig. 1. XRD patterns for $NiO/MgAl_2O_4$ and NiO/CeO_2-$K/MgAl_2O_4$.

that a small amount of carbon deposition was observed in the reactor, also below 700 °C where the conversion was low, indicating that thermal decomposition of 2-methylfuran forming coke also occurred.

Steam reforming of 2-methylfuran was investigated at temperatures between 400 and 700 °C over Ni/CeO_2-$K/MgAl_2O_4$ at a S/C-ratio of 5. The product yields and conversion of 2-methylfuran as function of temperature can be seen in Fig. 2. The main products at all temperatures were CO, CO_2, CH_4, and H_2 and as expected from thermodynamics, the yield of CO increased with increasing temperature, while the yield of CO_2 and CH_4 decreased with temperature. The yield of H_2 had a maximum of 76% at 600 °C (note our definition of yield, which is based on the fraction of converted reactant, Eq. (12)), while the conversion increased with increasing temperature, reaching full conversion at 700 °C. The product fraction called Others in Fig. 2 includes various compounds like ethanol, acetone, acetaldehyde, 2-butanone, and furan, which all are fragments of 2-methylfuran. This fraction decreased with temperature from a yield of 7% at 400 °C to 0% at 600 °C. Ethanol and acetone were the major constituents of the fraction Others and reached maximum yields of 0.8 and 1.5% respectively at 400 °C. However, the conversion was only 20% at 400 °C and therefore the production of these compounds were quite low.

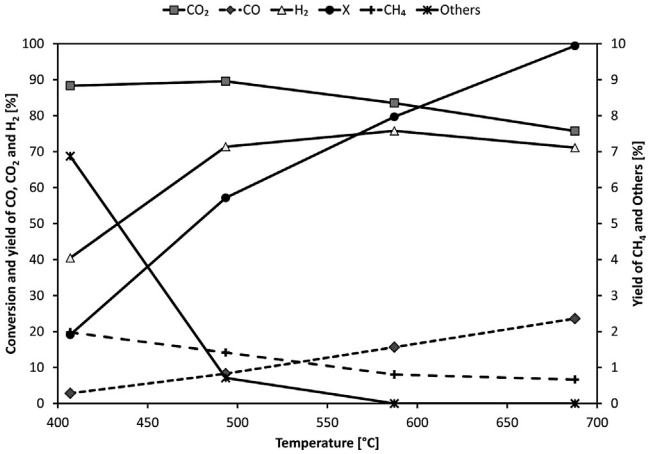

Fig. 2. Yield of CO, CO_2, CH_4, H_2, Others, and conversion as function of temperature over Ni/CeO_2-$K/MgAl_2O_4$ in the SR of 2-methylfuran. Experimental conditions: S/C: 5.2, m_{Cat} = 0.50 g, Ni loading: 8.2 wt%, F_T = 1.6 NL/min, y_{2MF} = 1.4 vol%, y_{H_2O} = 37.5 vol%, N_2 as balance.

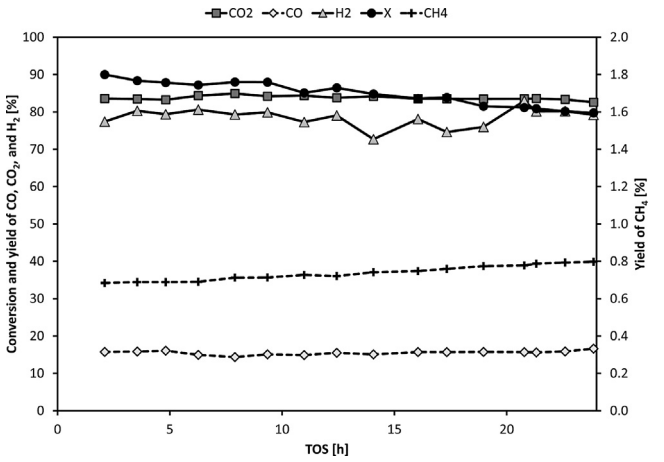

Fig. 3. Yield of CO, CO_2, CH_4, H_2, and conversion as function of time in SR of 2-methylfuran over Ni/CeO_2-$K/MgAl_2O_4$. Experimental conditions: S/C: 5.2, m_{Cat} = 0.50 g, Ni loading: 8.2 wt%, Temp.: 584 °C, F_T = 1.6 NL/min, y_{2MF} = 1.4 vol%, y_{H_2O} = 37.5 vol%, N_2 as balance.

The conversion of 2-methylfuran over Ni/CeO_2-$K/MgAl_2O_4$ and yields of CO, CO_2, CH_4, and H_2 as function of time at 584 °C and S/C = 5 can be seen in Fig. 3. The yield of H_2 was around 80%, while the conversion started at 90% and decreased to 80% over 24 h. The product yields of CO, CO_2, and CH_4 remained quite stable with time-on-stream.

A comparison of final conversion and carbon deposition at 584 °C and S/C = 5 for different times on stream and over both $Ni/MgAl_2O_4$ or Ni/CeO_2-$K/MgAl_2O_4$ can be seen in Table 2. After 4 h on stream, the conversion of 2-methylfuran was 12%-points lower and the carbon deposition was 7 times higher over $Ni/MgAl_2O_4$ compared with Ni/CeO_2-$K/MgAl_2O_4$, which shows the beneficial effect of adding both CeO_2 and K to the catalyst. This was also shown in a study of SR of ethanol [17].

A comparison of the conversion over Ni/CeO_2-$K/MgAl_2O_4$ after 4 h and 24 h on stream shows that the catalyst deactivated rather slowly with time, see Table 2. This was probably due to carbon deposition, which increased at a constant rate of 8 mg C/g_{Cat} h. The low rate of deactivation and rather constant rate of carbon deposition indicates that the carbon may be deposited as whiskers as discussed later [40,41,66,67].

The release of carbon oxides as function of temperature during TPO of spent Ni/CeO_2-$K/MgAl_2O_4$-catalysts used in the SR of 2-methylfuran at SR- and oxidative SR-conditions can be seen in Fig. 4. The carbon oxides release rate over a catalyst used in the SR at S/C = 5 had a maximum at 410–420 °C, which was similar to the observations from the TPO of spent catalyst used in the SR of ethanol [17]. A much smaller carbon oxides release peak was observed at 650 °C. This was not seen in the SR of ethanol and could correspond to carbon deposition on the reactor walls. Carbon deposits were observed visually on the walls of the reactor used in the SR

Table 2
Final conversion and carbon deposition over $Ni/MgAl_2O_4$ and Ni/CeO_2-$K/MgAl_2O_4$ in the SR of 2-methylfuran. Experimental conditions: S/C: 5.2, m_{Cat} = 0.50 g, Ni loading: 8.2 wt%, Temp.: 584 °C, F_T = 1.6 NL/min, y_{2MF} = 1.4 vol%, y_{H_2O} = 37.5 vol%, N_2 as balance.

Catalyst	TOS	X	Carbon deposition		
	[h]	[%]	[mmol C/mol C_{Feed}]	[mg C/g_{Cat} h]	[mg]
$Ni/MgAl_2O_4$	4	74	7.7	60	121
Ni/CeO_2-$K/MgAl_2O_4$	4	86	1.1	8	16
Ni/CeO_2-$K/MgAl_2O_4$	24	79	1.1	8	99

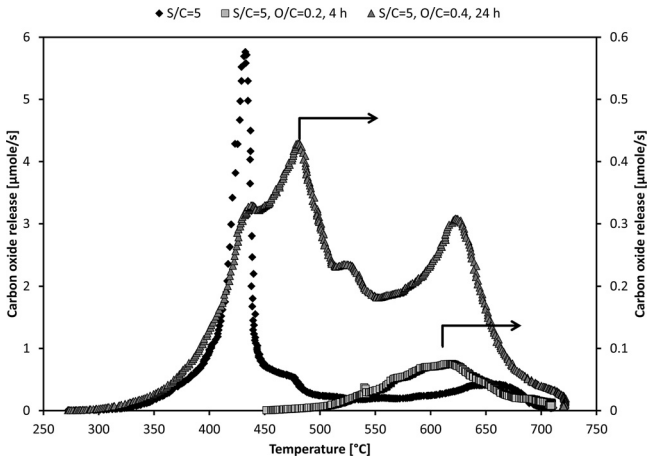

Fig. 4. Release of carbon oxides as function of temperature over Ni/CeO_2-K/$MgAl_2O_4$ after 4 h at SR conditions and 4 and 24 h at OSR conditions with 2-methylfuran as reactant. Experimental conditions: heating rate = 10 °C/min, F_T = 1 NL/min, y_{O_2} = 2 − 3 vol%, N_2 as balance.

of 2-methylfuran, but not in the SR of ethanol. Carbon whiskers was observed in the SR of ethanol over Ni/CeO_2-K/$MgAl_2O_4$ [17] and together with the stable behavior with time and the similar TPO-profiles this suggests that the carbon deposition was as carbon whiskers in the SR of 2-methylfuran.

Oxidative SR of ethanol can minimize carbon deposition [31] and therefore the SR of 2-methylfuran was investigated under oxidative conditions at O/C-ratio of 0.4. The conversion of 2-methylfuran and the yields of CO, CO_2, CH_4, and H_2 as function of time at 600 °C, S/C = 5, and O/C = 0.4 can be seen in Fig. 5. The conversion remained at 100% during the 4 h experiment, while the yield of CH_4 and H_2 was stable at roughly 0.4% and 68%, respectively, which was lower compared with the yields at SR-conditions. The product yields of CO and CO_2 were also stable with time. No formation of other compounds was observed.

A comparison of conversion, carbon deposition, yield of H_2 and CH_4 after 4 h and 24 h on stream in the OSR and 24 h in the SR of 2-methylfuran can be seen in Table 3. The addition of O_2 to the feed increased the conversion to 100% and therefore the mass of catalyst was lowered from 0.5 g to 0.39 g in the 24 h OSR experiment to see if less than full conversion could be achieved. However, full conversion was still reached, while the carbon deposition and yield

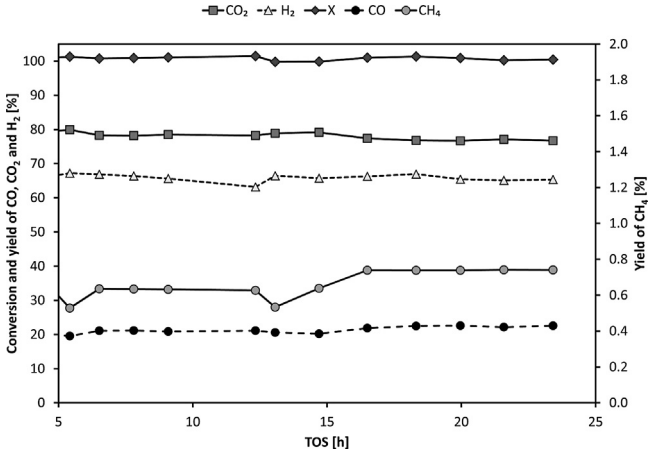

Fig. 5. Yield of CO, CO_2, CH_4, H_2, and conversion as function of time in OSR of 2-methylfuran over Ni/CeO_2-K/$MgAl_2O_4$. Experimental conditions: S/C: 5.1, m_{Cat} = 0.50 g, Ni loading: 8.2 wt%, Temp.: 600 °C, F_T = 1.6 NL/min, y_{2MF} = 1.5 vol%, y_{H_2O} = 37.8 vol%, y_{O_2} = 1.3 vol%, N_2 as balance.

Table 3
Final conversion, yield of H_2 and CH_4, and carbon deposition after 24 h on stream in SR of 2-methylfuran and after 4 and 24 h in the OSR of 2-methylfuran over Ni/CeO_2-K/$MgAl_2O_4$. Experimental conditions: S/C: 5.1, O/C: 0–0.4, m_{Cat} = 0.50 g for SR and OSR, m_{Cat} = 0.39 g for OSR (High SV), Ni loading: 8.2 wt%, Temp.: 584 °C, F_T = 1.6 NL/min, y_{2MF} = 1.4–1.5 vol%, y_{H_2O} = 37.5–38.0 vol%, y_{O_2} = 0 − 1.5 vol%, N_2 as balance.

Type	TOS	X	Y_{H_2}	Y_{CH_4}	Carbon deposition	
	[h]	[%]	[%]	[%]	mmol C/mol C_{Feed}	[mg C/g_{Cat} h]
SR	24	82	81	0.7	1.1	8.2
OSR	4	100	68	0.4	0.046	0.35
OSR (high SV)	24	100	66	0.7	0.058	0.6

of H_2 still were lower compared with SR at S/C = 5. The fraction of feed being converted to carbon deposits decreased by a factor of 18 from 1.1 mmol C/mol C_{Feed} to 0.06 mmol C/mol C_{Feed}, showing that oxygen addition is effective in minimizing carbon deposition in SR of oxygenates.

The product yields were stable in the 24 h experiment, but the yield of CH_4 was slightly higher compared with the 4 h experiment. This was probably due to the lower mass of catalyst, which did not allow for the same degree of conversion of CH_4. The rate of carbon deposition was similar after 4 h and 24 h, when comparing the fraction of the feed converted to carbon deposition, mmol C/mol C_{Feed}.

The release of carbon oxides during TPO of the catalysts used in the oxidative SR of 2-methylfuran for 4 and 24 h are shown in Fig. 4. The rate of carbon oxidation had a maximum at roughly 610 °C after 4 h on stream, indicating that the carbon was not deposited on CeO_2, K, or Ni as these compounds catalyze the oxidation leading to oxidation at lower temperatures [17,68–70]. The carbon oxides release above 500 °C in SR was roughly 4 times as high as the carbon oxides release observed in OSR of 2-methylfuran after 4 h. This indicates that the oxygen addition decreases both the carbon deposition on the catalyst and on the reactor walls.

After 24 h of operation the carbon oxidation occurred over a broader temperature range and with several peaks at 430 °C, 480 °C, 520 °C, and 620 °C, which indicates that carbon was deposited on the catalytic particles as well as surfaces with little or no catalytic activity. This shows that not only the amount of carbon deposits changes with time, but also the type and/or position of the deposited carbon.

3.3. Steam reforming of furfural

The product yields of CO, CO_2, CH_4, H_2, Others, and conversion of furfural as function of temperature in the SR of furfural at S/C = 5 are summarized in Fig. 6. The conversion increased with temperature from 12% at 400 °C to 96% at 700 °C, while the yield of H_2 had a maximum of 85% at 600 °C, however only slightly higher compared to yields at 500 and 700 °C. The yield of CO increased with temperature while the yield of CO_2 had a maximum at 500 °C. The trends in the yield of CO and CO_2 at 500 °C and above are as expected based on thermodynamics as they predict that the WGS (reaction (2)) shifts toward the left with increasing temperature. The apparent maximum in yield of CO_2 at 500 °C is because furfural is mainly converted to hydrocarbons at lower temperatures. The yield of by-products called Others was 19% at 400 °C and decreased to less 0.1% at 500 °C. The fraction Others consisted of 90% of ethanol and 2-propanol in a ratio of 10:1, while acetic acid, butanoic acid, and hydrofuranes made up the remaining 10%. Similar products were observed by Xu et al. [62]. Hydrofuranes are formed by hydrogenation of the furan-ring, while ethanol and 2-propanol are fragments of furfural. The yield of CH_4 had a maximum of 0.2% at 500 °C, which was significantly lower compared with the yield of CH_4 in the

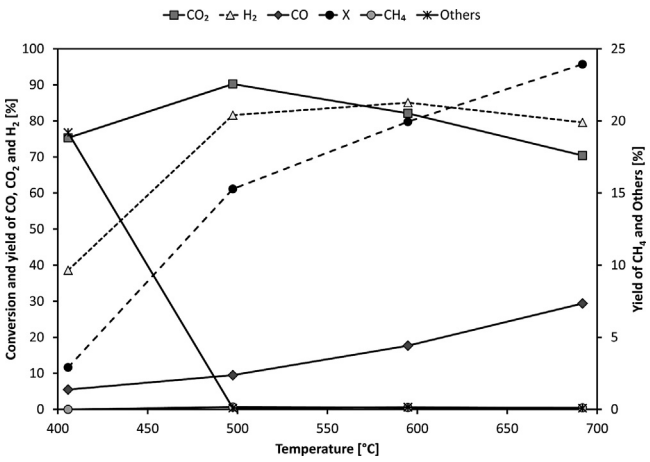

Fig. 6. Yield of CO, CO_2, CH_4, H_2, Others, and conversion as function of temperature in the SR of furfural over Ni/CeO_2-K/$MgAl_2O_4$. Experimental conditions: S/C: 5.0, m_{Cat} = 0.50 g, Ni loading: 8.2 wt%, F_T = 1.6 NL/min, y_{FF} = 1.5 vol%, y_{H_2O} = 38.7 vol%, N_2 as balance.

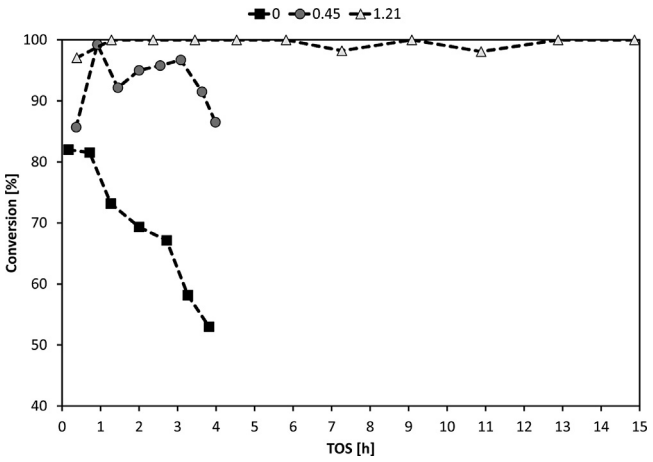

Fig. 8. Conversion as function of time in SR of furfural over Ni/CeO_2-K/$MgAl_2O_4$ at different O/C-ratios. Experimental conditions: S/C: 5.0–5.3, m_{Cat} = 0.50 g, Ni loading: 8.2 wt%, Temp.: 584–616 °C, F_T = 1.6 NL/min, y_{FF} = 1.4–1.5 vol%, y_{H_2O} = 38.0–38.4 vol%, y_{O_2} = 0–4.8 vol%, N_2 as balance.

SR of 2-methylfuran. 2-methylfuran has a methyl group in the 2-position on the furan ring, where furfural has a carbonyl group. The higher yield of CH_4 in the SR of 2-methylfuran is probably related to the methyl-group, which easily can be converted to methane by reaction with adsorbed H.

The conversion of furfural and the product yields of CO, CO_2, CH_4, and H_2 as function of time in the SR of furfural at 600 °C and S/C = 5 can be seen in Fig. 7. The product distribution was quite stable with time-on-stream although a slight decrease in the yield of H_2 from 61% to 57% was observed. However, the conversion decreased significantly from 82% to 53% during 4 *h* on stream. The much faster rate of deactivation compared with SR of 2-methylfuran was apparent in the rate of carbon deposition, which was 66 mg C/g_{Cat} h compared to 8 mg C/g_{Cat} h in the SR of 2-methylfuran at similar conditions.

Oxidative SR of furfural was investigated at two different O/C-ratios. The O/C-ratio of 0.4 used in the SR of 2-methylfuran was not high enough to induce a high and stable conversion and therefore a higher O/C-ratio of 1.2 was investigated as well. The conversion as function of time-on-stream at the different O/C-ratios can be seen in Fig. 8. Full conversion was achieved at O/C-ratio of 1.2 and it remained stable for 15 h.

The yield of H_2 and hydrocarbons as well as conversion and carbon deposition after 4 h on stream as function of O/C-ratio can be seen in Fig. 9. Similar to the observations in the SR of 2-methylfuran under oxidative conditions the yield of H_2 and carbon deposition decreased while the conversion increased. The yield of hydrocarbons shown in Fig. 9 includes methane, ethene, ethane, and propene, and surprisingly increased with increasing O/C-ratio. Generally a higher conversion is expected to lead to lower yields of hydrocarbons, as they are intermediates in the SR reactions. The opposite trend observed here could be due to partial oxidation of the Ni-particles as increasing amounts of O_2 are fed to the reactor along with a low production of H_2, which may not be enough to keep the catalyst fully reduced. To investigate this hypothesis, an initially unreduced Ni/CeO_2-K/$MgAl_2O_4$ catalyst was tested in SR of furfural and the results are shown versus time in Fig. S.2. It can be seen that the yield of hydrocarbons was initially high (20%) and then decreased to zero after 1 h while the carbon oxides and H_2 started to form. This indicates that hydrocarbons are important by-products over the non-reduced catalyst, and that oxidation of the catalyst is responsible for the observed increasing amount of hydrocarbons at increasing O/C level. It may be noticed that an unreduced

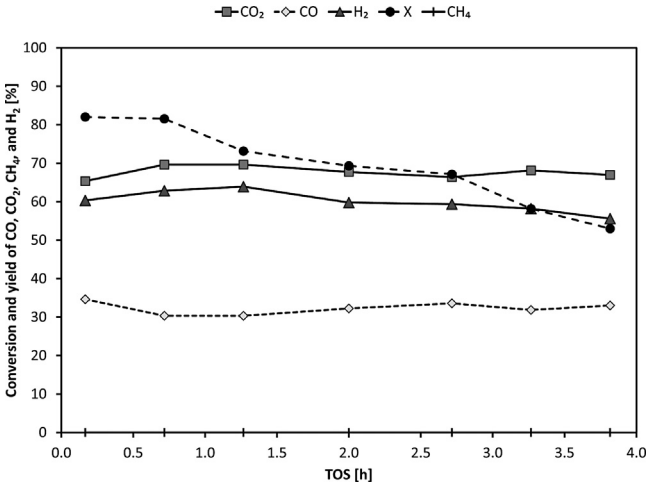

Fig. 7. Yield of CO, CO_2, CH_4, H_2, and conversion as function of time in the SR of furfural over Ni/CeO_2-K/$MgAl_2O_4$. Experimental conditions: S/C: 5.1, m_{Cat} = 0.50 g, Ni loading: 8.2 wt%, Temp.: 584 °C, F_T = 1.6 NL/min, y_{FF} = 1.4 vol%, y_{H_2O} = 38.0 vol%, N_2 as balance.

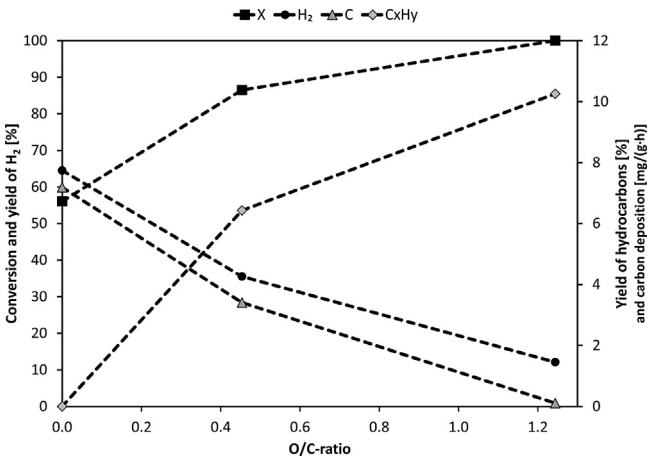

Fig. 9. Conversion, carbon deposition, yield of H_2 and hydrocarbons as function of O/C-ratio in SR of furfural over Ni/CeO_2-K/$MgAl_2O_4$ after 4 h on stream. Hydrocarbons include methane, ethene, ethane, and propene. Experimental conditions: TOS: S/C: 5.0–5.3, m_{Cat} = 0.50 g, Ni loading: 8.2 wt%, Temp.: 584–616 °C, F_T = 1.6 NL/min, y_{2MF} = 1.4–1.5 vol%, y_{H_2O} = 38.0–38.4 vol%, y_{O_2} = 0–4.8 vol%, N_2 as balance.

Table 4
Product yields, conversion, and carbon deposition after 4 and 24 h in OSR of furfural. Experimental conditions: S/C: 5.0–5.3, O/C: 1.2, m_{Cat} = 0.50 g, Ni loading: 8.2 wt%, Temp.: 584–616 °C, F_T = 1.6 NL/min, y_{FF} = 1.4–1.5 vol%, y_{H_2O} = 38.0–38.4 vol%, y_{O_2} = 4.8 vol%, N_2 as balance.

TOS	[h]	4	24
Yield			
CO	[%]	23	34
CO_2	[%]	67	56
CH_4	[%]	5	2
C_2H_4	[%]	4	7
C_3H_7	[%]	1	1
H_2	[%]	24	14
X	[%]	100	100
C_{Dep}	[mmol C/mol C_{Feed}]	0.11	6.2
C_{Dep}	[mg C/g_{Cat} h]	0.34	18.6

$Ni/MgAl_2O_4$ catalyst is not able to catalyze any reactions and this catalyst therefore does not self-reduce. This shows that K and CeO_2 either increases the reducibility of NiO or has enough SR activity to produce H_2 to initiate the reduction of NiO.

Steam reforming of furfural at O/C = 1.2, S/C = 5.2, and 600 °C was conducted for 24 h and a comparison of product yields, conversion, and carbon deposition after 4 h and 24 h on stream can be seen in Table 4. The conversion was 100% both after 4 and 24 h, but the yield of ethene increased, while the yield of H_2 decreased showing deactivation of the catalyst. Furthermore, the CO_2/CO-ratio decreased with time indicating a loss in WGS activity. The deactivation was also apparent in the rate of carbon deposition, which increased drastically from 0.11 mmol C/mol C_{Feed} after 4 h to 6.2 mmol C/mol C_{Feed} after 24 h, i.e. roughly a factor of 50.

The release of carbon oxides as function of temperature during TPO of the catalyst after 4 h at SR conditions and after 4 and 24 h at OSR conditions can be seen in Fig. 10. The carbon oxides release after 4 h at SR conditions showed one distinct oxidation peak at 410 °C, which probably is due to oxidation of carbon in contact with K, Ni, and/or CeO_2, similar to the observations in the SR of 2-methylfuran. Carbon oxidation was also observed in the range of 600–700 °C, which could be due to oxidation of carbon deposits on material with little or no catalytic activity like the reactor walls, $MgAl_2O_4$, and on top of the catalyst bed [71]. The carbon oxides release during TPO of two empty reactors used in SR of furfural are shown in Fig. S.3 in the Supporting Information. This figure shows carbon oxidation at 400–450 °C and at 500–650 °C, where the oxidation at high temperatures could correspond to carbon on reactor

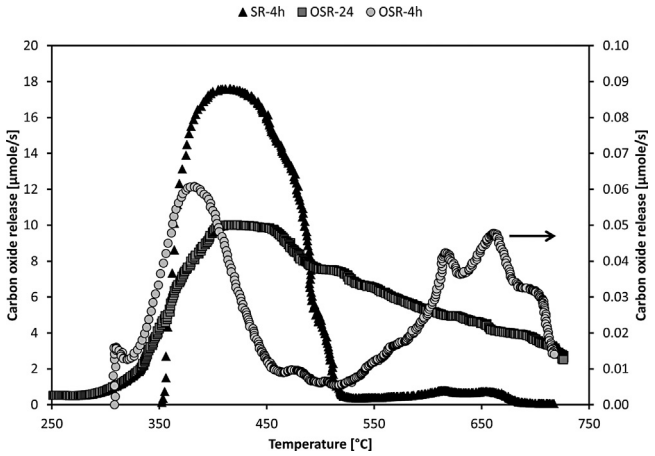

Fig. 10. Carbon oxides release as function of temperature over Ni/CeO_2-K/$MgAl_2O_4$ after 4 h at S/C = 5 and 4 h and 24 h at S/C = 5 and O/C = 1.2 in the SR of furfural. Experimental conditions: heating rate = 10 °C/min, F_T = 1 NL/min, y_{O_2} = 2–3 vol%, N_2 as balance.

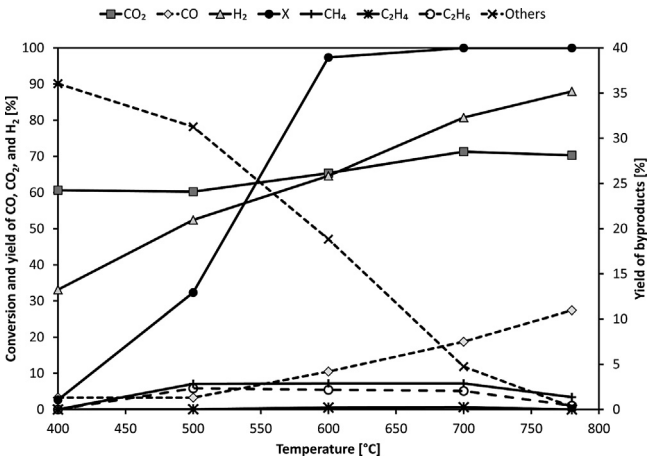

Fig. 11. Yield of CO, CO_2, CH_4, C_2H_4, C_2H_6, H_2, Others, and conversion as function of temperature in the SR of guaiacol over Ni/CeO_2-K/$MgAl_2O_4$. Experimental conditions: S/C: 5.2, m_{Cat} = 0.50 g, Ni loading: 8.2 wt%, F_T = 1.6 NL/min, y_{GUA} = 1.1 vol%, y_{H_2O} = 38.1 vol%, N_2 as balance.

wall, while the oxidation at the low temperatures indicates that a more reactive carbon form also was deposited. It should be noted that the majority of the carbon deposition is on the catalysts since carbon oxides release from the empty reactors only corresponds to 1% of the total carbon deposition on the catalyst and reactor.

The carbon oxides release peaks at 600–700 °C were observed in the SR and OSR after 4 h, but was lower in OSR. This indicates that the oxygen decreases carbon deposition on both catalytic and uncatalytic materials, similar to the observations in the SR and OSR of 2-methylfuran. The carbon oxides release after 24 h at OSR conditions showed one broad peak from 300 to 750 °C with a maximum at 415 °C, indicating carbon deposits on both materials with and without catalytic activity. The large increase in the rate of carbon deposition from 4 to 24 h as well as the change in oxidation profile could indicate an induction period and after which the rate of carbon deposition might reach a constant rate, similar to the observations in SR of 2-methylfuran.

3.4. Steam reforming of guaiacol

Steam reforming of guaiacol was investigated at S/C = 5 and the conversion and product yields as function of temperature are summarized in Fig. 11. The conversion, yield of H_2, and yield of CO all increased with increasing temperature, while the yield of CO_2 remained at a value of 60–70% at all temperatures. The yield of H_2 had a maximum of 88% at 780 °C, while full conversion was reached at 700 °C and above. Besides the expected products, CO, CO_2, CH_4, and H_2, also ethene and ethane were produced in a ratio of 1:10 at all temperatures. The high formation of ethane was unlike any of the other compounds investigated. Benzenediols and phenol were produced in high yields and these compounds constituted the major part (70–80%) of the product fraction Others shown in Fig. 11. The high yields of these compounds indicate that the removal of the methyl group from guaiacol is facile. The yield of benzenediols and phenol as function of temperature can be seen in Fig. S.4 in the Supporting Information. The yield of Others, methane, ethane, and ethene all decreased with increasing temperature. The yield of Others was quite high even at 700 °C, which indicates that the activation and conversion of aromatic compounds requires high temperature. Full conversion with a yield of Others below 0.5% was achieved at 780 °C, which was significantly higher compared with furfural and 2-methylfuran.

The conversion and product yields as function of time-on-stream in the SR of guaiacol at 600 °C and S/C = 5 can be seen in

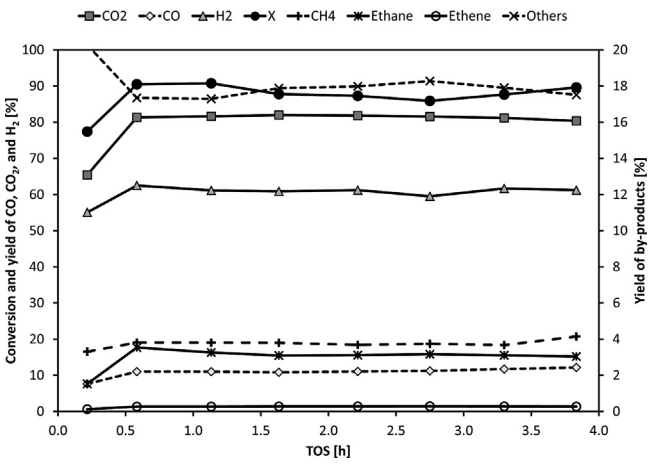

Fig. 12. Product yields and conversion as function of time in SR of guaiacol over Ni/CeO_2-K/$MgAl_2O_4$. Experimental conditions: S/C: 5.1, m_{Cat} = 0.50 g, Ni loading: 8.2 wt%, Temp.: 584 °C, F_T = 1.6 NL/min, y_{2MF} = 1.4 vol%, y_{H_2O} = 38.0 vol%, N_2 as balance.

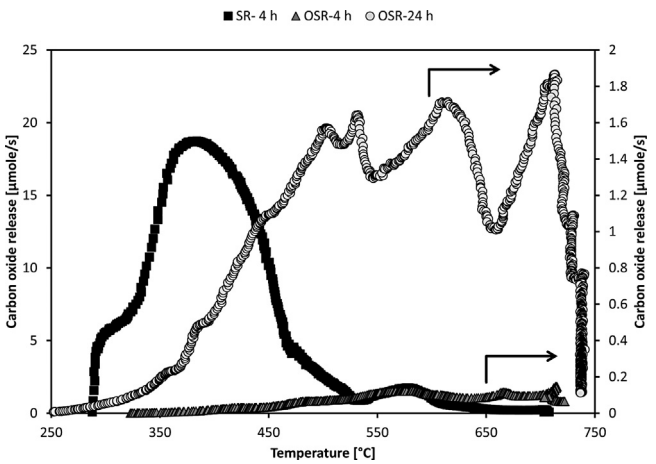

Fig. 13. Carbon oxides release as function of temperature over Ni/CeO_2-K/$MgAl_2O_4$ after 4 h at SR and OSR conditions and 24 h at OSR conditions with guaiacol as reactant. SR and OSR at 600 °C, S/C: 5.2–5.4, and O/C: 0.80–0.83. Experimental conditions: Heating rate = 10 °C/min, F_T = 1 NL/min, y_{O_2} = 2–3 vol%, N_2 as balance.

Fig. 12. The yield of H_2 and conversion remained stable at 61% and 90%, respectively, for the entire experiment. Despite the stable behavior, there was still observed significant carbon deposition at a rate of 73.5 mg C/g_{Cat} h, see Table 5. This indicates that the carbon was deposited as whiskers.

Oxidative SR of guaiacol at S/C = 5 and O/C = 0.8 was tested for 4 h and 24 h, and the conversion and the products yields at the end of each experiment is compared with the results from SR of guaiacol after 4 h at 600 °C in Table 5. The beneficial effect of adding O_2 is observed for SR of guaiacol as well as for the other compounds, as the conversion increased, while the carbon deposition was decreased significantly, again at the expense of the yield of H_2.

Full conversion was achieved both after 4 and 24 h on stream at OSR conditions. However, the product distribution showed signs of catalyst deactivation as the yield of H_2 decreased while the yield of by-products increased. Furthermore the rate of carbon deposition increased by a factor of 3 from 4 h to 24 h on stream.

The carbon oxides release as function of temperature after 4 h at SR conditions and 4 h and 24 h at OSR conditions can be seen in Fig. 13. The carbon oxides release after 4 h at SR-conditions occurred in single peak at 410 °C with a shoulder at 580 °C similar to the other investigated compounds. The carbon oxides release during TPO of an empty reactor after use in the SR of guaiacol is compared with the TPO-profile from SR of guaiacol (incl. catalyst) in Fig. S.5 in the Supporting Information. The empty reactor showed carbon oxides release at 560 °C indicating that the shoulder is related to carbon deposited on the reactor walls. Furthermore the amount of carbon deposited in the empty reactor was 10% of total carbon deposition. This was higher compared to the SR of furfural, which indicates that the thermal decomposition of guaiacol is more severe.

The TPO profiles of the spent catalysts used in OSR of guaiacol suggest that the main part of carbon deposition was on the reactor walls or other materials with little or no catalytic activity as the carbon oxides release was mainly at 600 °C and above and not at 410–420 °C as expected for catalyzed carbon oxidation. The carbon oxides release after 24 h in OSR was higher and moved toward lower temperatures indicating that the catalytic particles were covered by carbon with time-on-stream, which could also explain the increase in the rate of carbon deposition.

Further increments of the O/C-ratio is probably needed to obtain a stable product distribution and suppress carbon deposition in the SR of guaiacol and furfural at 600 °C.

3.5. Postreaction characterization

Catalysts, which have been used in the SR of furfural at S/C = 5, SR of guaiacol at S/C = 5, or SR of guaiacol at S/C = 5 and O/C = 0.8 at roughly 600 °C and for 4 h, were characterized by XRD and TEM. The XRD patterns of the spent catalysts used in the SR of furfural and guaiacol at S/C = 5 can be seen in Fig. S.6 in the Supporting Information. XRD analysis of the spent catalysts from SR of furfural and guaiacol showed an additional peak at 52° compared with the XRD pattern of the fresh catalyst, which corresponds to the reflection peak from metallic Ni.

The NiO and CeO_2 particle size of the fresh and spent catalyst, estimated by XRD, can be seen in Table 6. Sintering was not significant in SR at S/C = 5 as the Ni particles had the same size as the fresh catalyst.

Table 5
Product yields, conversion, and carbon deposition after 4 and 24 h in OSR of guaiacol. Experimental conditions: S/C: 5.2–5.4, O/C: 0.80–0.83, m_{Cat} = 0.50 g, Ni loading: 8.2 wt%, Temp.: 584–616 °C, F_T = 1.6 NL/min, y_{GUA} = 1.0 − 1.1 vol%, y_{H_2O} = 38.2–39 vol%, y_{O_2} = 0–3.1 vol%, N_2 as balance.

Type		SR	OSR	OSR
TOS	[h]	4	4	24
Yield				
CO	[%]	12.2	16.1	19.6
CO_2	[%]	80.4	80.5	76.3
CH_4	[%]	4.2	2.2	1.9
C_2H_4	[%]	0.3	0.2	0.2
C_2H_6	[%]	3.0	1.0	1.0
Others	[%]	13.7	0.9	5.1
H_2	[%]	64	54	48
X	[%]	86	100	100
C_{Dep}	[mmol C/mol C_{Feed}]	9.9	0.2	0.6
C_{Dep}	[mg C/g_{Cat} h]	73.5	1.3	4.5

Table 6
Particle size of NiO and CeO_2 crystals on fresh and spent Ni/CeO_2-K/$MgAl_2O_4$-catalysts used in the SR of furfural and guaiacol at SR and oxidative SR conditions for 4 h and 24 h.

	NiO [nm]	CeO_2 [nm]
Fresh	7	6
SR of furfural, S/C = 5	6	7
SR of guaiacol, S/C = 5	6	8
OSR of guaiacol, S/C = 5, O/C = 0.8, 4 h	17	6
OSR of guaiacol, S/C = 5, O/C = 1.2, 24 h	17	6

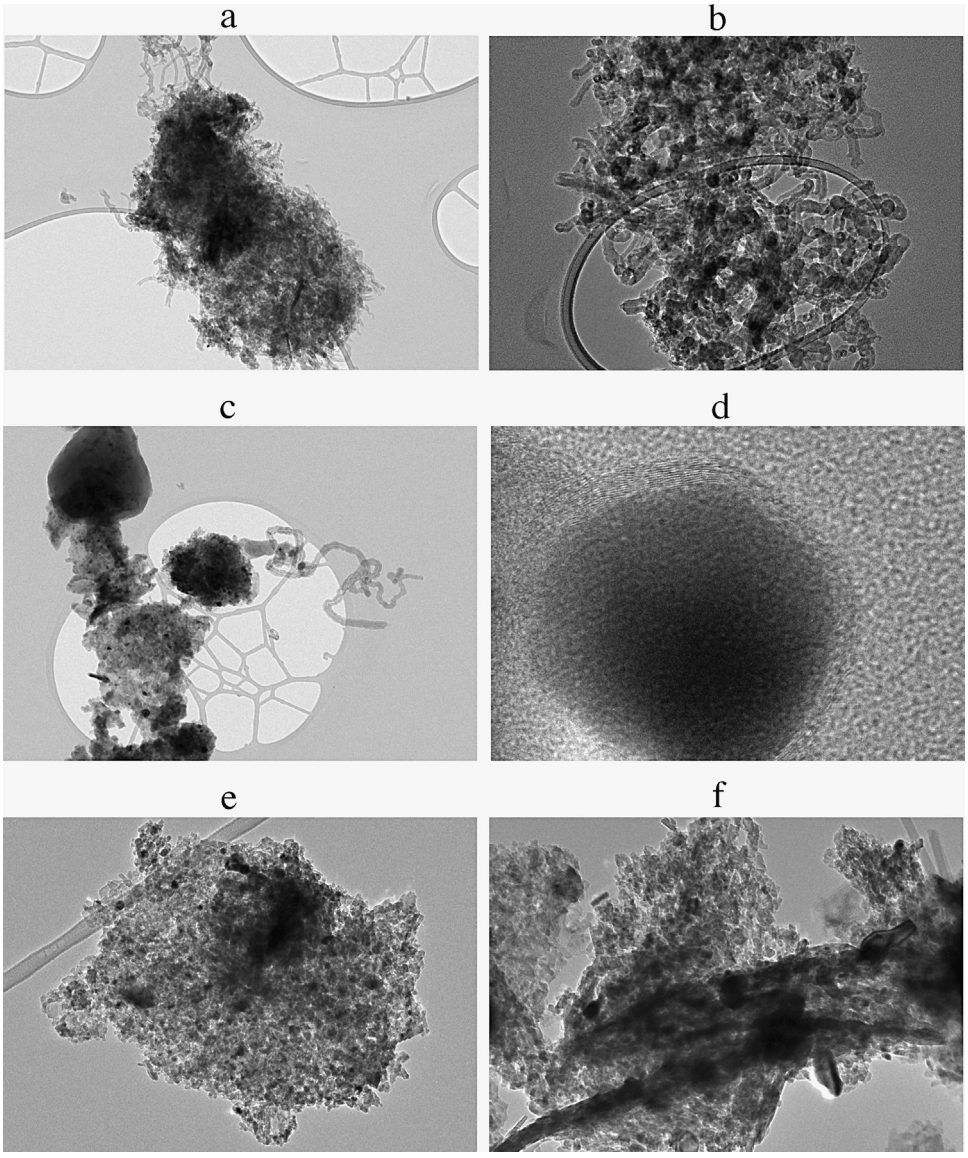

Fig. 14. TEM images of spent Ni/CeO_2-$K/MgAl_2O_4$-catalysts used in the SR of furfural and guaiacol at SR and OSR conditions at 600 °C.

The XRD patterns of spent catalysts used in the SR of guaiacol at S/C = 5 and O/C = 1.2 for 4 h and 24 h are shown in Fig. S.7 in the Supporting Information. The peaks from NiO were higher and sharper for these catalysts, which indicate that the NiO particles sintered and the particle sizes were estimated to be roughly 17 nm. Thus, sintering was more pronounced in oxidative SR, which also has been shown in the SR and oxidative SR of ethanol [31]. The sintering of the particles in oxidative SR did not significantly increase with time-on-stream as XRD analysis of spent catalysts, which had been operated for 24 h in the SR of guaiacol had a similar NiO particle diameter as for 4 h of operation, see Table 6.

Sintering of the CeO_2 was not observed neither under SR conditions nor oxidative SR conditions, as shown in Table 6.

The sintering observed in OSR may explain the accelerated rate of carbon deposition with time, as the larger particles may be more susceptible to carbon deposition compared with smaller particles. Therefore the carbon deposition might accelerate, as the particles grow to a certain size, after which the carbon deposition rate stabilizes at a high value.

TEM images of the spent catalysts used in OSR and SR at 600 °C can be seen in Fig. 14. Carbon whiskers were formed in quite large amounts in the SR of furfural and guaiacol at S/C = 5 as shown in Fig. 14a and c. This indicates that the carbon oxidation at 400–430 °C is related to the carbon whiskers. Carbon deposition as encapsulating gum was observed in the SR of guaiacol, which can be seen in Fig. 14d as a layer on the surface of the metal particles, and in Fig. 14c as large dark areas [27]. The encapsulating carbon was present is lower amounts and it could correspond to the carbon oxidized at temperatures above 500 °C.

No formation of carbon whiskers was observed on the catalyst, which had been used in the oxidative SR of guaiacol, as indicated in Fig. 14e and f. However, indications of carbon deposition as encapsulating gum were still observed in Fig. 14f. This also implies that the carbon oxidized at high temperatures is encapsulating carbon as carbon oxidation was mainly observed at temperatures above 550 °C in oxidative SR of guaiacol after 4 h on stream.

EDX-analysis of the spent catalyst indicated that the loading of K, Ni, and CeO_2 was 3.2 wt%, 7.8 wt%, and 4.7 wt%, respectively, which was close to the nominal loading indicated in Table 1. This indicates that there is no significant loss of K during the experiments.

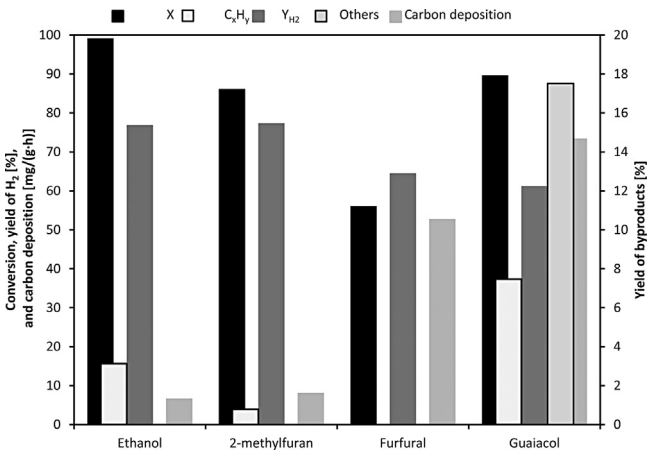

Fig. 15. Conversion, carbon deposition, yield of H_2, by-products (Others), and hydrocarbons after 4 h on stream for the ethanol, 2-methylfuran, furfural, and guaiacol in SR over Ni/CeO_2-K/$MgAl_2O_4$ at 600 °C and S/C-ratio of 5–6. Experimental conditions: S/C: 5.2, m_{Cat} = 0.50 g, Ni loading: 8.2 wt%, F_T = 1.6 NL/min, y_{Oxy} = 1.1–3.0 vol%, y_{H_2O} = 36.5–38.1 vol%, N_2 as balance.

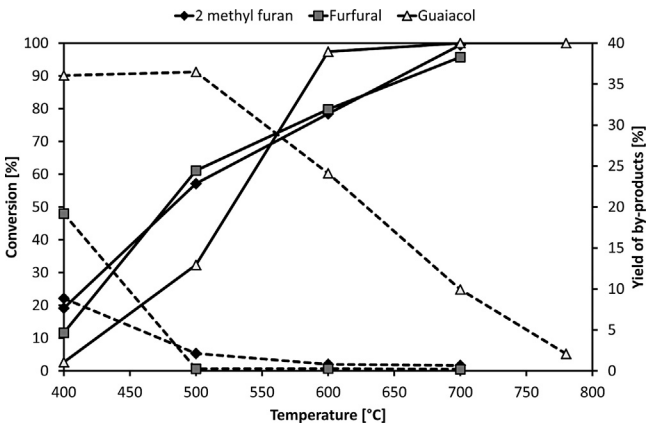

Fig. 16. Conversion and yield of by-products as function of temperature in the SR of 2-methylfuran, furfural, and guaiacol in SR over Ni/CeO_2-K/$MgAl_2O_4$ at S/C-ratio of 5. Solid lines are conversion while dotted lines are yield of by-products. Experimental conditions: S/C: 5.0–5.2, m_{Cat} = 0.50 g, Ni loading: 8.2 wt%, F_T = 1.6 NL/min, y_{Oxy} = 1.1–1.5 vol%, y_{H_2O} = 38.1 vol%, N_2 as balance.

3.6. Comparison of SR of different oxygenates

Steam reforming of different cyclic model compounds of bio-oil has been investigated in this study and a comparison of conversion, carbon deposition, yield of H_2, by-products, and hydrocarbons after 4 h on stream in the SR of ethanol (data from [31]), 2-methylfuran, furfural, and guaiacol at 600 °C and S/C-ratio of 5–6 can be seen in Fig. 15. The conversion was lower for all the cyclic compounds compared to ethanol. The carbon deposition was highest for guaiacol followed by furfural, while 2-methylfuran and ethanol had similar rates of carbon deposition. The larger cyclic compounds thus were less reactive and had a higher tendency to form carbon deposits compared with ethanol. Similar results have been reported by Hu and Lu [59] for the SR of glucose, *m*-xylene, ethyl acetate, acetone, ethylene glycol, and acetic acid.

The only structural difference between furfural and 2-methylfuran is that furfural has a carbonyl group in the 2-position on the furan-ring, while 2-methylfuran has a methyl group. This indicates that the increased rate of carbon deposition in the SR of furfural compared to the SR of 2-methylfuran is related to the carbonyl group. A possible explanation could be self condensation reactions of furfural leading to carbon deposition and catalyst deactivation. Another explanation for the differences in carbon deposition could be differences in the formation of olefins, like ethene or propene, but this was not observed in this study.

The aromatic nature of guaiacol is probably responsible for the high rate of carbon deposition observed in the SR of guaiacol compared to furfural and especially ethanol and 2-methylfuran. The yield of H_2 was similar in the SR of ethanol and 2-methylfuran and higher compared to the yield obtained in the SR of guaiacol and furfural. Significant amounts of by-products were mainly observed in the SR of guaiacol and ethanol, and was mainly methane in the SR of ethanol and large fractions of both CH_4, C_2H_6, and aromatic compounds in the SR of guaiacol.

The conversion and total yield of byproducts as function of temperature for the cyclic model compounds can be seen in Fig. 16. The conversion as function of temperature was similar for 2-methylfuran and furfural which is expected as the two model compounds have similar structures. The conversion of guaiacol was lower compared to the other model compounds at 400 and 500 °C indicating that high temperatures are needed to activate the aromatic ring. At 600 °C the total conversion was higher for guaiacol, but the yield of by-products was still high (24%), so the conversion to the desired products was lower compared with furfural and 2-methylfuran. Overall the results show that the conversion of guaiacol requires higher temperature and furthermore that the carbon deposition in the SR of guaiacol is the highest of all the investigated compounds showing that guaiacol and probably also other phenolics are more difficult to steam reform.

4. Conclusions

Steam reforming of three different model compounds of the cyclic oxygenates in bio-oil, 2-methylfuran, furfural, and guaiacol, have been investigated at S/C-ratio of 5 and temperatures between 400 and 800 °C over Ni/CeO_2-K/$MgAl_2O_4$. The conversion, yield of H_2, and CO increased with increasing temperature, while the yield of CO_2 and by-products decreased with increasing temperature for all the model compounds. The major products at all temperatures were carbon oxides (CO and CO_2) and H_2, but small hydrocarbons, like methane and ethene, as well as fragments of the model compounds, like acetone, ethanol, phenol, were also observed in the effluent. This was most pronounced for guaiacol, where a yield of aromatic by-products of 17% at 97% conversion was observed at 600 °C. Temperatures of 700 °C were needed to fully convert 2-methylfuran and furfural to carbon oxides and H_2, while temperatures above 780 °C were required in the SR of guaiacol.

Significant carbon deposition was observed for all the model compounds and it was highest for guaiacol followed by furfural and 2-methylfuran. TEM-images showed that the carbon deposited as carbon whiskers at SR conditions. Sintering of Ni or CeO_2 was not observed at SR-conditions.

The carbon deposition could be significantly decreased by adding oxygen to the feed at a O/C-ratio between 0.2 and 1.2. The oxygen addition increased the conversion and full conversion, with low yields of by-products, could be achieved at 600 °C. The beneficial effects of oxygen addition were at the expense of a significant decrease in the yield of H_2. The actual decrease in the yield of H_2 depended on the model compound and the applied O/C-ratio. Furthermore significant sintering of the Ni-particles was observed in oxidative SR as well as an increase in the rate of carbon deposition with time on stream. Stable behavior was not achieved over 24 h in the oxidative SR of furfural and guaiacol.

Overall, the results indicate that SR of oxygenates is very challenging and is even more so for aromatic compounds. Furthermore the results indicate that the only path to stable operation with no

carbon deposition is through oxidative SR although here sintering may be a challenge.

Acknowledgments

This work is part of the CHEC (Combustion and Harmful Emission Control) Research Center, EGSSE (European Graduate School of Sustainable Energy), and CASE (Catalysis for Sustainable Energy). The present work is financed by The Technical University of Denmark. Thomas Willum Hansen from DTU CEN is gratefully acknowledged for assistance with TEM measurements.

Appendix A. Supplementary data

Supplementary data associated with this article can be found, in the online version, at http://dx.doi.org/10.1016/j.apcatb.2014.09.026.

References

[1] G.W. Huber, S. Iborra, A. Corma, Chem. Rev. 106 (2006) 4044–4098.
[2] P. Gallezot, A. Kiennemann, Handbook of Heterogeneous Catalysis, Wiley-VCH, 2010, pp. 2447–2476.
[3] K. Raffelt, E. Henrich, A. Koegel, R. Stahl, J. Steinhardt, F. Weirich, Appl. Biochem. Biotechnol. 129 (2006) 153–164.
[4] A. Oasmaa, Y. Solantausta, V. Arpiainen, E. Kuoppala, K. Sipilä, Energy Fuels 24 (2010) 1380–1388.
[5] R.H. Venderbosch, W. Prins, Biofuel. Bioprod. Bioref. 4 (2010) 178–208.
[6] W. Kwapinski, C.M.P. Byrne, E. Kryachko, P. Wolfram, C. Adley, J.J. Leahy, et al., Waste Biomass Valor 1 (2010) 177–189.
[7] T.N. Trinh, P.A. Jensen, K. Dam-Johansen, K.N. Knudsen, H.R. Sørensen, S. Hvilsted, Energy Fuels 27 (2013) 1399–1409.
[8] A. Oasmaa, S. Czernik, Energy Fuels 13 (1999) 914–921.
[9] A. Oasmaa, D. Meier, J. Anal. Appl. Pyrolysis 73 (2005) 323–334.
[10] A. Demirbas, Appl. Energy 88 (2011) 17–28.
[11] P.M. Mortensen, J.-D. Grunwaldt, P.A. Jensen, K.G. Knudsen, A.D. Jensen, Appl. Catal. A: Gen. 407 (2011) 1–19.
[12] R. Trane, A.D. Jensen, S. Dahl, Int. J. Hydrogen Energy 37 (2012) 6447–6472.
[13] R. Rioche, S. Kulkarni, F.C. Meunier, J.P. Breen, R. Burch, Appl. Catal. B: Environ. 61 (2005) 130–139.
[14] A.C. Basagiannis, X.E. Verykios, Int. J. Hydrogen Energy 32 (2007) 3343–3355.
[15] M. Ni, D. Leung, M. Leung, Int. J. Hydrogen Energy 32 (2007) 3238–3247.
[16] A. Haryanto, S. Fernando, N. Murali, S. Adhikari, Energy Fuels 19 (2005) 2098–2106.
[17] R. Trane-Restrup, S. Dahl, A.D. Jensen, Int. J. Hydrogen Energy 38 (2013) 15105–15118.
[18] A.C. Basagiannis, X.E. Verykios, Appl. Catal. B: Environ. 82 (2008) 77–88.
[19] J. Sun, X.-P. Qiu, F. Wu, W.-T. Zhu, Int. J. Hydrogen Energy 30 (2005) 437–445.
[20] X. Hu, G. Lu, J. Mol. Catal. A: Chem. 261 (2007) 41–48.
[21] E.C. Vagia, A.A. Lemonidou, J. Catal. 269 (2010) 388–396.
[22] F. Bimbela, D. Chen, L. Garcìa, J. Arauzo, Appl. Catal. B: Environ. 119–120 (2012) 1–12.
[23] L. De Rogatis, T. Montini, B. Lorenzut, P. Fornasiero, Energy Environ. Sci. 1 (2008) 501–509.
[24] E.C. Vagia, A.A. Lemonidou, Appl. Catal. A: Gen. 351 (2008) 111–121.
[25] J.R. Salge, G.A. Deluga, L.D. Schmidt, J. Catal. 235 (2005) 69–78.
[26] X. Hu, G. Lu, Catal. Commun. 12 (2010) 50–53.
[27] J. Rass-Hansen, C.H. Christensen, J. Sehested, S. Helveg, J.R. Rostrup-Nielsen, S. Dahl, Green Chem. 9 (2007) 1016–1021.
[28] N.R. Peela, A. Mubayi, D. Kunzru, Chem. Eng. J. 167 (2011) 578–587.
[29] N.R. Peela, D. Kunzru, Int. J. Hydrogen Energy 36 (2011) 3384–3396.
[30] X. Hu, G. Lu, Green Chem. 11 (2009) 724–732.
[31] R. Trane-Restrup, S. Dahl, A.D. Jensen, Int. J. Hydrogen Energy 39 (2014) 7735–7746.
[32] W. Cai, F. Wang, C. Daniel, A.C. van Veen, H. Provendier, C. Mirodatos, J. Catal. 286 (2012) 137–152.
[33] S.M. de Lima, A.M. da Silva, L.O. de Costa, J.M. Assaf, L.V. Mattos, F.B. Noronha, et al., Appl. Catal. B: Environ. 121 (2012) 1–9.
[34] G.A. Deluga, J.R. Salge, L.D. Schmidt, X.E. Verykios, Science 303 (2004) 993–997.
[35] C.-C. Hung, S.-L. Chen, Y.-K. Liao, C.-H. Chen, J.-H. Wang, Int. J. Hydrogen Energy 37 (2012) 4955–4966.
[36] J.A. Medrano, M. Oliva, J. Ruiz, L. Garcìa, J. Arauzo, Int. J. Hydrogen Energy 33 (2008) 4387–4396.
[37] L. Schmidt, R. French, S. Czernik, T. Josephson, D. Rennard, Int. J. Hydrogen Energy 35 (2010), 4048–1059.
[38] J.A. Medrano, M. Oliva, J. Ruiz, L. Garcìa, Energy 36 (2011) 2215–2224.
[39] X. Hu, G. Lu, Int. J. Hydrogen Energy 35 (2010) 7169–7176.
[40] J.R. Rostrup-Nielsen, L.J. Christiansen, Concepts in Syngas Manufacture, Imperial College Press, 2011.
[41] J.R. Rostrup-Nielsen, J. Catal. 33 (1974) 184–201.
[42] R. Trane-Restrup, D.E. Resasco, A.D. Jensen, Catal. Sci. Technol. 3 (2013) 3292–3302.
[43] P.D. Vaidya, A.E. Rodrigues, Chem. Eng. J. 117 (2006) 39–49.
[44] P. Lan, Q. Xu, M. Zhou, L. Lan, S. Zhang, S. Yan, Chem. Eng. Technol. 33 (2010) 2021–2028.
[45] P. Lan, Q.-L. Xu, L.-H. Lan, D. Xie, S.-P. Zhang, Y.-J. Yan, Energy Sources A 34 (2012) 2004–2015.
[46] J. Remon, J.A. Medrano, F. Bimbela, L. Garcìa, J. Arauzo, Appl. Catal. B: Environ. 132–133 (2013) 433–444.
[47] D. Wang, S. Czernik, E. Chornet, Energy Fuels 12 (1998) 19–24.
[48] Q. Xu, P. Lan, B. Zhang, Z. Ren, Y. Yan, Energy Fuels 24 (2010) 6456–6462.
[49] S. Czernik, R. Evans, R. French, Catal. Today 129 (2007) 265–268.
[50] S. Czernik, R. French, C. Feik, E. Chornet, Ind. Eng. Chem. Res. 41 (2002) 4209–4215.
[51] L. Garcìa, R. French, S. Czernik, E. Chornet, Appl. Catal. A: Gen. 201 (2000) 225–239.
[52] A.C. Basagiannis, X.E. Verykios, Catal. Today 127 (2007) 256–264.
[53] P.N. Kechagiopoulos, S.S. Voutetakis, A.A. Lemonidou, I.A. Vasalos, Energy Fuels 20 (2006) 2155–2163.
[54] H. Li, Q. Xu, H. Xue, Y. Yan, Renew. Energy 34 (2009) 2872–2877.
[55] S. Liu, M. Chen, L. Chu, Z. Yang, C. Zhu, J. Wang, M. Chen, Int. J. Hydrogen Energy 38 (2013) 3948–3955.
[56] B. Valle, A. Remiro, A.T. Aguayo, J. Bilbao, A.G. Gayobo, Int. J. Hydrogen Energy 38 (2013) 1307–1318.
[57] M. Marquevich, S. Czernik, E. Chornet, D. Montane, Energy Fuels 13 (1999) 1160–1166.
[58] D. Wang, S. Czernik, D. Montane, M. Mann, E. Chornet, Ind. Eng. Chem. Res. 36 (1997) 1507–1518.
[59] X. Hu, G. Lu, Appl. Catal. B: Environ. 88 (2009) 376–385.
[60] C.M. Roggero, V. Tumiatti, A. Scova, C. De Leo, A. Binello, G. Cravetto, Energy Sources A 33 (2011) 467–476.
[61] C. Wu, Q. Huang, M. Sui, Y. Yan, F. Wang, Fuel Process. Technol. 89 (2008) 1306–1316.
[62] Q. Xu, D. Xie, F. Wang, Y. Yan, Energy Sources A: Recov. Utiliz. Environ. Eff. 35 (2013) 1028–1038.
[63] S. Sayas, A. Chica, Int. J. Hydrogen Energy 39 (2014) 5234–5241.
[64] P. Gallezot, G. Bergeret, Handbook of Heterogeneous Catalysis, Wiley-VCH, 2010, pp. 738–765.
[65] H.S. Fogler, Elements of Chemical Reaction Engineering, 4th ed., Prentice Hall, 2006.
[66] D.L. Trimm, Catal. Today 37 (1997) 233–238.
[67] D.L. Trimm, Catal. Today 49 (1999) 3–10.
[68] R.J. Gorte, React. Kinet. Catal. 56 (2010) 1126–1135.
[69] C.F. Oliveira, F.A.C. Garcia, D.R. Araujo, J.L. Macedo, J.L. Dias, S.C.L. Dias, Appl. Catal. A: Gen. 413–414 (2012) 292–300.
[70] C.A. Neyertz, E.E. Miro, C.A. Querini, Chem. Eng. J. 181–182 (2012) 93–102.
[71] A. Remiro, B. Valle, A.T. Aguayo, J. Bilbao, Gayubo, Fuel Process. Technol. 115 (2013) 222–232.